

On some factors influencing the laboratory measurement of permeability of rock

A. GŁOWACKI* and A. P. S. SELVADURAI*

The paper presents the results of one-dimensional laboratory permeability experiments conducted on three rock types: limestone, granite and sandstone. The experiments investigate how sample preparation, saturation and flow reversal can influence the attainment of a steady pressure gradient. The results show that the peak pressure gradient recorded in an experiment can be related to the residual pressure gradient that can be used to estimate the permeability of rocks.

KEYWORDS: laboratory tests; permeability

ICE Publishing: all rights reserved

NOTATION

A	cross-sectional area of the sample normal to the one-dimensional flow direction
K	permeability
L	length of the sample
p_i, p_o	fluid inlet and outlet pressures, respectively
p_i^{\max}, p_i^{\min}	inlet peak pressure and inlet stable pressure, respectively
Q	flow rate
γ_w	unit weight of the permeating fluid
μ	dynamic viscosity of water
ϕ	porosity defined as the volume of voids divided by the total volume of sample
Ω	pressure differential threshold
ω	proportionality constant

INTRODUCTION

Accurate estimates of permeability of rocks can influence geotechnical and geo-environmental activities associated with geological disposal of hazardous materials, groundwater management, resource exploration and the development of material for infrastructure applications. Although the permeability of a rock is considered to be a unique property of its fabric and accessible pore space, in reality, several factors, including the fluid used in the experiments, the degree of saturation, movement of dislodged particles, chemical dissolution and erosion of the matrix, air bubble occlusion and the stress state, can significantly influence its measurement (Lee & Black, 1972; Wright *et al.*, 2002). However, these factors are typically not examined in great detail during the measurement of permeability in rock samples (Wang & Park, 2002; Zhang, 2013). Before conducting sophisticated experiments that involve triaxial stress states and temperature gradients, it is instructive to examine the permeability of unstressed rock samples. Such reference state experiments can provide insight into factors that can influence the interpretation of permeability from experimental data.

THEORETICAL RELATIONSHIPS

To describe the process of fluid flow through a porous medium by appeal to Darcy's law, the accessible pore space should be saturated by the permeating fluid and the flow velocities should be within the low Reynolds number range ($Re \leq 1$ or 10), where viscous forces are still dominant, to ensure laminar flow.

In the current experimental arrangements, the Bernoulli potential (Selvadurai, 2000) can be reduced to the pressure potential and the permeability can be estimated from the following relationship

$$K = \frac{Q\mu L}{A(p_i - p_o)} \quad (1)$$

where K is the permeability (L^2); Q is the flow rate (L^3/T); μ is the dynamic viscosity of water (M/TL); L is the length of the sample (L); A is the cross-sectional area of the sample normal to the one-dimensional flow direction (L^2); and the fluid pressures (M/TL^2) are prescribed at the inlet (p_i) and the outlet p_o boundaries of the one-dimensional region.

PREPARATION OF SAMPLES

Indiana limestone is a monomineralic rock consisting of calcite obtained from a quarry in Bedford, IN, USA. Stanstead granite is a medium to coarse-grained rock, typically found in the Beebe region of the Eastern Townships in Québec, Canada. The main minerals are quartz, feldspar laths, muscovite flakes and in small amounts biotite and chlorite (Najari, 2013). The Rudna sandstone samples were from the Rudna copper mine in Poland (Cieřlik, 2015). A chemical analysis indicates that it is primarily composed of quartz, dolomite and microcline. The exact in-situ depth and location of all samples used in this research are unknown; therefore the in-situ stress state is also unknown. The rocks could have been subjected to disturbance by extraction, transportation and handling.

The surfaces of the prepared samples were cleaned with water using a stainless steel brush to remove any debris produced by coring and machining. Typically, three layers of epoxy were applied to the surface (each layer was allowed to dry for 24 h), followed by the epoxying of the top and bottom acrylic caps (Fig. 1). Analysis of microscope images of thin sections of the interface between the rock and the epoxy indicated that the penetration of epoxy varied between 0.30 and 0.76 mm.

Manuscript received 12 September 2016; first decision 16 December 2016; accepted 17 December 2016.

Published online at www.geotechniqueletters.com on 11 January 2017.

*Department of Civil Engineering and Applied Mechanics, Environmental Geomechanics Laboratory, McGill University, Montréal, QC, Canada.

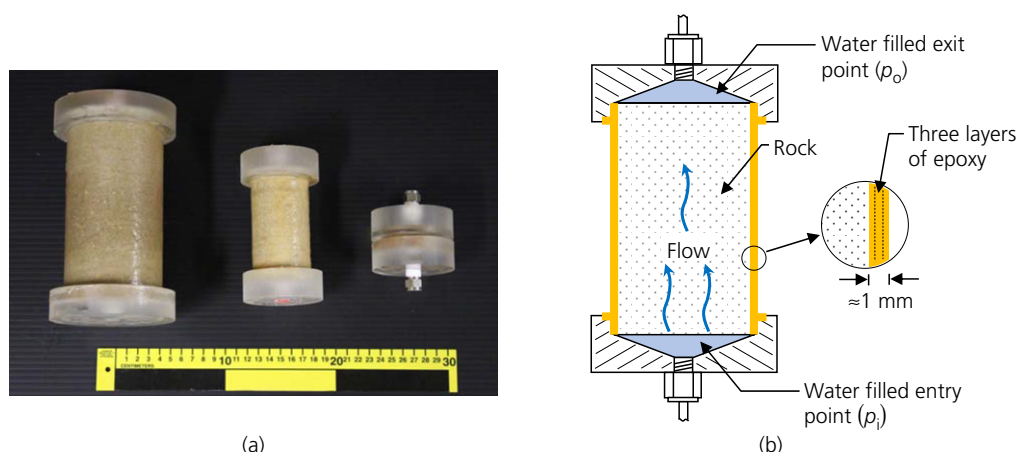


Fig. 1. (a) Indiana limestone samples epoxy coated and capped with acrylic caps; (b) typical cross-section of the caps, tapered to channel the water as well as to accommodate a national pipe threaded opening for connections

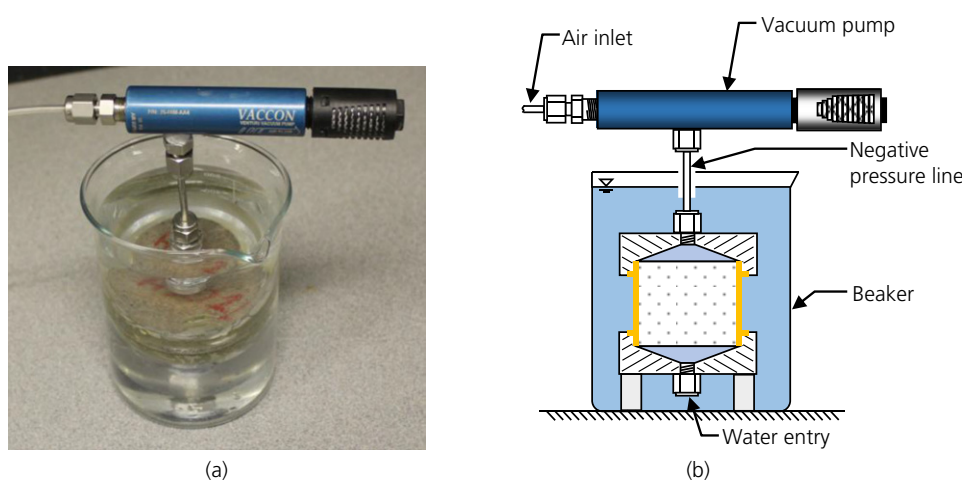


Fig. 2. (a) The vacuum saturation arrangement, where the sample is subjected to negative pressure (-81 kPa) at the top using a Venturi vacuum pump, (b) typical cross-section of the sample submerged in water

The assembled samples (i.e. with the acrylic caps and epoxy coating) were vacuum saturated using a Venturi pump at a vacuum pressure of -81 kPa (Fig. 2); the saturation was terminated when the water absorption, measured by periodic weighing, stabilised to within a change of 1% of the wet weight.

EXPERIMENTAL TECHNIQUE

In this paper, a series of uniaxial steady-state flow experiments (flow rates ranging from 0.1 to 0.01 ml/min) were conducted to examine the influence of (a) the initial degree of saturation, (b) flow reversal, (c) chemically altered water, (d) de-aired water, (e) debris from machining and (f) intermittent testing, on the estimation of permeability. The experimental arrangement involves the application of a pressure gradient to a cylindrical sample of rock to create a one-dimensional flow (Fig. 1).

A sample prepared in either a saturated or dry condition was connected to an in-line high-performance liquid chromatography pump using pipe fittings. The inflow pressure was monitored with a pressure transducer and the temperature was measured with a type-K thermocouple. The data were collected through a data acquisition system and stored on a laptop computer (Fig. 3).

Since the epoxy was applied manually, a single layer could potentially be of insufficient thickness to withstand the inflow pressure without interface delamination. For this reason, several complementary tests were carried out on rock samples to determine the number of layers necessary to achieve a proper seal. The pressure required to either delaminate or puncture the three epoxy layers was established by testing several samples of each rock type and performing a step-by-step increase in pressure until a break through pressure loss was recorded and leakage observed. The inflow pressure required to detach the three layers of epoxy coating was ~ 600 kPa. Typically, the pressure of the inflow was maintained at 50% (i.e. 300 kPa) of the epoxy delamination/puncture pressure. The inlet fluid pressures were kept below 10% of the tensile strength of the rock (tensile strengths of Stanstead granite: 8.4 MPa; Indiana limestone: 3.7 MPa; Rudna sandstone: 5.5 MPa) in order to avoid the creation of micro-cracks and/or damage to the samples. To ensure that mass conservation was satisfied and that no leakage occurred, the outflow water was weighed.

EXPERIMENTAL RESULTS

Results of experiments on initially dry samples

The permeabilities estimated from experiments conducted on air-dried samples are shown in Fig. 4. It was observed

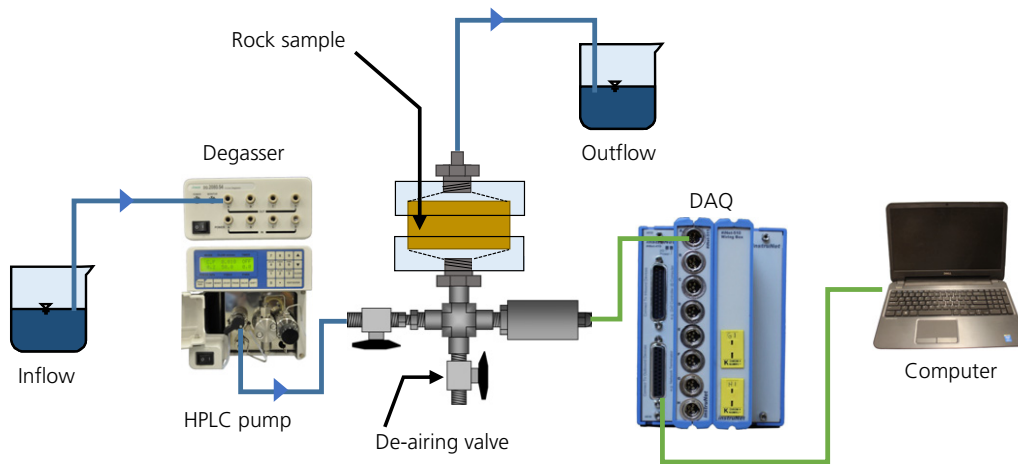


Fig. 3. Schematic view of the experimental arrangement

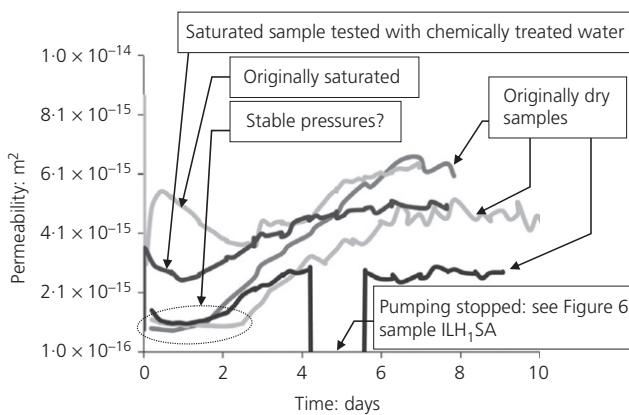


Fig. 4. Permeability against time, samples of Indiana limestone

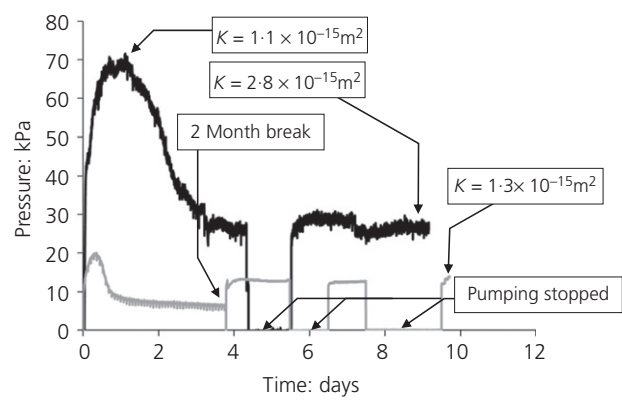


Fig. 6. Tests on Indiana limestone: time history of the inlet fluid pressure at the entry location [grey curve 0.1 ml/min flow rate, sample thoroughly brushed/washed to remove machining particulates; initially dry sample subjected to Venturi vacuum saturation with distilled helium de-aired water; after 2-month break, sample now saturated with distilled/de-aired water, ILH1SP4 (49.0 mm dia. 19.9 mm length); black curve 0.1 ml/min flow rate, distilled and helium de-aired water, initially dry sample, ILH1SA (50.2 mm dia. 98.9 mm height)]

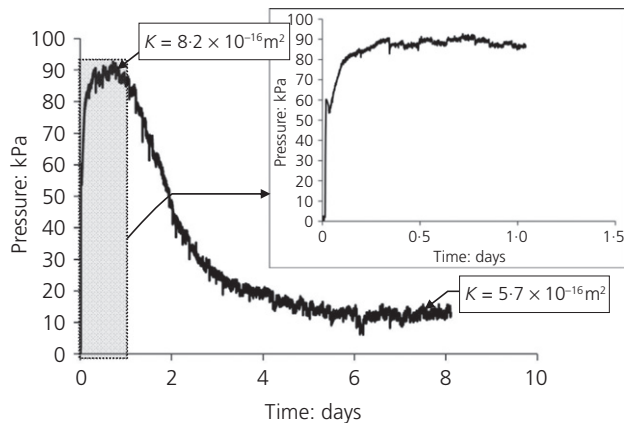


Fig. 5. Tests on Indiana limestone: time history of the inlet fluid pressure at the entry location [0.1 ml/min flow rate, distilled and helium de-aired water, initially dry sample, ILH1SC (50.24 mm dia. 98.9 mm length)]. The insert graph shows the short-term pressure history from the highlighted grey rectangle

that, irrespective of the rock type, the initially dry samples displayed an inlet water pressure that rose to a specific peak followed by a decay and finally the attainment of a steady pressure (Figs 5–8). For initially dry samples, it is particularly important to ascertain whether the recorded constant pressure gradient corresponds to a fully saturated condition.

The duration of the flow is not an assurance of full saturation since partial saturation can result from occluded air, pore space blockage and so on, and thus will lead to an erroneous estimation of permeability (see Fig. 4 between 0.5 and 2 days and Fig. 5) resulting in an error of around 86%.

Experiments on saturated samples

Saturated samples required between 2 and 4 days of continuous pumping to reach a plateau of stable pressure (Figs 7 and 8); in contrast, in some cases the initially dry rock samples took 21 days to reach equilibrium (Fig. 7). The difficulties encountered during the saturation process for rocks and the time required to reach 100% saturation (or near full saturation) are discussed in the work of Makhnenko & Labuz (2013). Furthermore, the initial peak pressure rise seen in the dry samples was either non-existent or reduced for the saturated samples.

The use of de-aired water

By using helium purging or degassing, the dissolved oxygen content in the water was reduced from 8 to 2 ppm and the

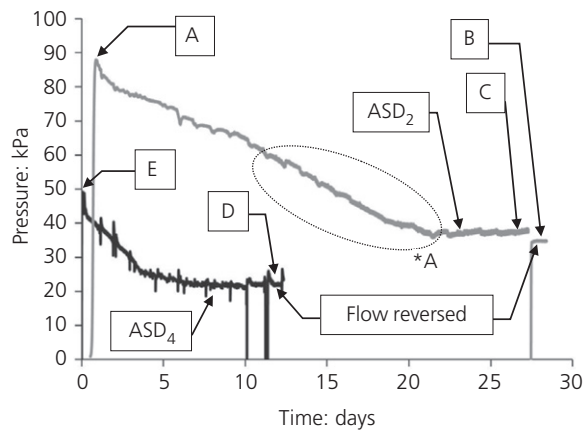


Fig. 7. Tests on Rudna sandstone: time history of the inlet fluid pressure at the entry location [0.01 ml/min flow rate, samples cleaned after machining by brushing under water, distilled/de-aired water; ASD2 sample, initially dry (51.03 mm dia. 27.15 mm length); ASD4 sample, 5 days vacuum (-81 kPa) saturated (51.1 mm dia. 18.87 mm length)]. Permeabilities at location: A, 2.3×10^{-17} m²; B, 5.8×10^{-17} m²; C, 5.4×10^{-17} m²; D, 6.3×10^{-17} m²; E, 3.1×10^{-17} m². Details of *A are shown in Fig. 9

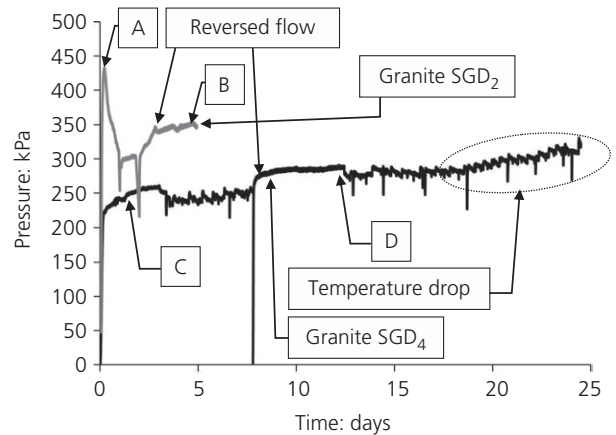


Fig. 8. Tests on Stanstead granite: time history of the inlet fluid pressure at the entry location [0.01 ml/min flow rate, samples were cleaned after machining by brushing under water, distilled/de-aired water; SGD2 initially dry sample (50.2 mm dia., 20.04 mm length); SGD4, 7 days vacuum (-81 kPa) saturated sample (50.2 mm in dia., 18.8 mm length)]. Permeability at A: 3.5×10^{-18} m²; B: 4.3×10^{-18} m²; C: 5.0×10^{-18} m²; D: 5.7×10^{-18} m²

number of pressure peak fluctuations due to the functioning of the pump pistons decreases significantly (Dolan, 1999). The use of oxygen-deprived water during permeability testing allows the water to flush out, absorb and retain air bubbles that may occlude the interconnected flow paths and facilitates pore space saturation, since water can retain up to 2% per volume of dissolved air (Fredlund, 1976). The air bubbles that were initially visible on the top surface of the acrylic cap dissolved into the de-aired water, confirming that this is an efficient method for removing air bubbles.

Results from experiments using disodium phosphate (Na_2HPO_4) at 14 ppm and calcium carbonate (CaCO_3) at 47 ppm saturated water

The results on Indiana limestone did not yield any conclusive evidence about the influence of the chemical composition of water on the stabilisation of the inlet pressure (i.e. it did not eliminate the pressure response 'spikes' nor did it significantly affect the estimated permeability of the rock).

Results of chemical analysis of the outflow

The results indicate that the measured dissolution of the rock matrix with distilled/de-aired water has no significant impact on the estimated permeability, within the time (several days) of testing; are similar to those obtained from tests conducted using either chemically treated water or normal water.

Results of experiments with no flow for extended periods of time

Figure 6 presents data for experiments on Indiana limestone where pumping with a stabilised inlet pressure was stopped for a period of ~ 36 h, in order to verify whether any time-dependent chemical process could influence permeability estimation or whether the attained pressures were stable and repeatable when the pumping was resumed. The samples were not allowed to dry out during this period, and once pumping resumed, the pressures stabilised to previous values, confirming that such rest periods had no influence on the estimation of permeability.

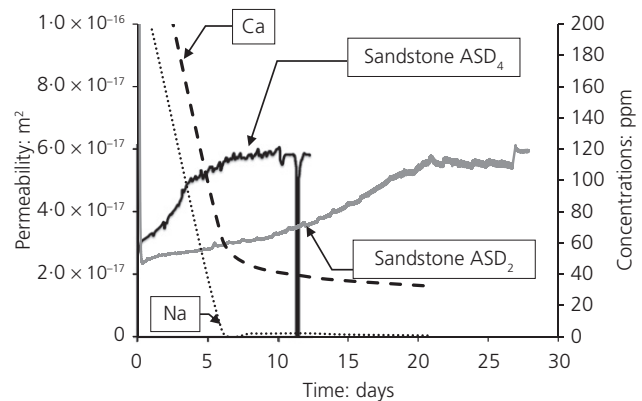


Fig. 9. Permeability against time against outflow concentration for Rudna sandstone samples; chemical analysis of outflow for calcium and sodium was done on the initially dry sample ASD2

Results of experiments conducted by reversing the flow direction

The effect of reversing the fluid flow direction on the estimation of permeability was examined (Figs 9 and 10). Flow reversal and recharge in boreholes are common during groundwater recharge and backwashing. For granite and sandstone, reversing the inflow had only a minor effect on the inlet fluid pressures (Figs 7 and 8). However, these minor pressure changes (-4% for sandstones, $+12\%$ for granites) indicate that there is some evidence of particulate movement within the flow channels even at the scale of the 20 mm long and 50 mm dia. samples. The results obtained from an Indiana limestone sample with machining/coring debris on both entry and exit surfaces indicate that the clogging of pores, which results in discontinuities in the pressure-time history, are observed even when a steady pressure was attained.

A correlation between peak and residual steady-state hydraulic gradients

An observation in these studies is that the attainment of a steady-state hydraulic gradient necessary for the estimation of the permeability of different types of rock will be

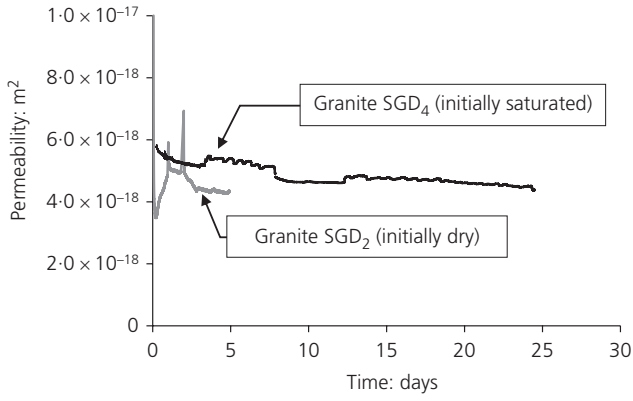


Fig. 10. Permeability against time, Stanstead granite samples

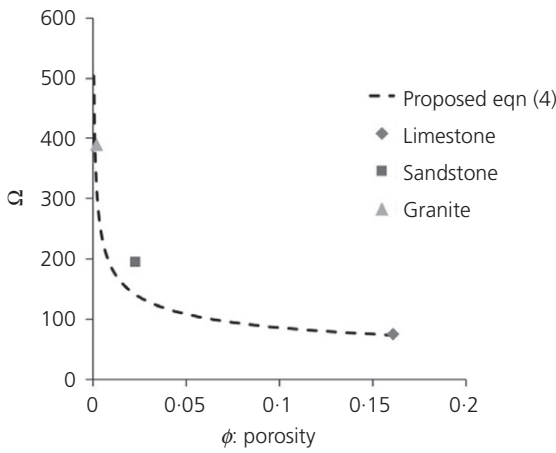


Fig. 11. Pressure adjustment factor against porosity showing the trend for three types of rock

influenced by a number of factors with the initial degree of saturation exerting the greatest influence. With the initially dry samples, the inlet pressure develops a peak (p_i^{\max}) and with progressive saturation reaches a stable threshold (p_i^{\min}). It is conjectured that $(p_i^{\max} - p_i^{\min})$ is proportional to the length of the drainage path (L) (i.e. the longer the draining path the greater the differential threshold) and inversely proportional to the porosity (ϕ) of the rock (i.e. the lower the porosity the greater the differential threshold), which gives the following relationship

$$(p_i^{\max} - p_i^{\min}) \propto \frac{L}{f(\phi)} \quad (2)$$

where $f(\phi)$ is an arbitrary function of the porosity. If it is assumed that each rock that is tested is an idealised porous medium that is chemically uninfluenced by the permeating fluid, then the results obtained for the separate rock types can be regarded as being applicable to three porosity measures (averaged for each rock type). Considering the experimental data, it can be shown that the non-dimensional pressure differential threshold Ω defined by

$$\Omega = \frac{(p_i^{\max} - p_i^{\min})}{\gamma_w L} \quad (3)$$

is related to the porosity according the empirical relationship

$$\Omega = \frac{40}{\sqrt[3]{\phi}} \quad (4)$$

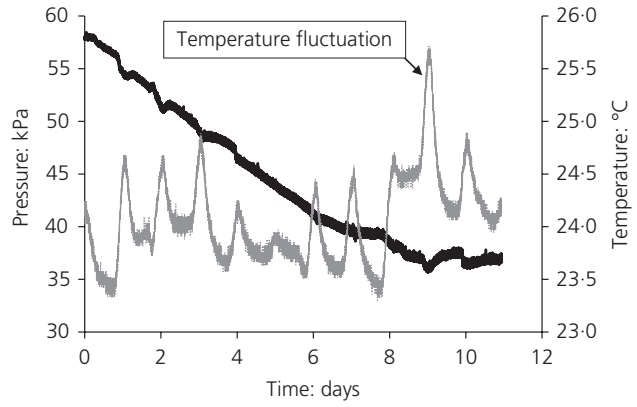


Fig. 12. Tests on Rudna sandstone: time history of the inlet fluid pressure at the entry location against temperature of water for ASD2; the black curve is the zoomed-in region *A shown in Fig. 7; the grey curve is the temperature

The correlation is shown in Fig. 11. For example: In order to use equation (4), the specific sample porosity, length and peak inflow pressure are required. In Fig. 5, for the sample ILH1SC (50.24 mm dia., 98.9 mm length), with a porosity 0.16 and a peak pressure of 90 kPa, equations (3) and (4) would yield a stabilised pressure value (p_i^{\min}) of 16 kPa.

DISCUSSIONS AND CONCLUSIONS

The common trend observed in the permeability tests on unsaturated specimens was a rise in the inflow pressure to a peak value followed by a steady, lengthy decay to a stable value. From the results of this research, for the initially dry samples, a new empirical relationship is proposed to predict the final steady-state inflow pressure, which can be used to estimate the saturated permeability. The ability to predict the ultimate steady-state inlet pressure under steady flow conditions will reduce the time required to conduct steady-state tests.

The results also raise questions about the use of the vacuum saturation procedure since in some cases, the initial peak pressures were not avoided by vacuum saturating the samples (i.e. see Fig. 7: Rudna sandstone).

When analysing the results it was noticed that the temperature has a noticeable effect on the inflow pressure response (i.e. an increase in temperature results in viscosity reduction and a decrease in the inflow pressure, Figs 8 and 12). These effects can be minimised by monitoring and maintaining a constant room temperature or by submerging the fittings and the sample in a water bath (ideally the temperature variation of water should be $\pm 1^\circ\text{C}$).

The sample preparation can influence the results in terms of the presence of debris from machining that could clog the flow paths, which leads to unstable inlet pressures. The results from flow reversal tests demonstrate that there is a change in pressure gradients in sandstone and in granite once steady-state conditions have occurred.

ACKNOWLEDGEMENTS

The work was supported by NSERC and NWMO research grants awarded to Professor A.P.S. Selvadurai. The authors thank Mr John Bartczak, Senior Technician, Civil Engineering Laboratory, McGill University for his valuable assistance and expertise in preparing the experimental facilities. The first author is grateful for the studentship support provided by a McGill Engineering Doctoral Award, FQRNT and the SAAQ. Reports containing the physical,

mechanical and chemical properties of the rocks tested can be obtained by contacting the authors.

REFERENCES

- Cieślak, J. (2015). Stress drop as a result of splitting brittle and transitional faulting of rock samples in uniaxial and triaxial compression tests. *Stud. Geotech. Mech.* **37**, No. 1, 17–23.
- Dolan, J. W. (1999). Mobile-phase degassing – why, when, and how. *LCGC North America*, 1 October: pp. 908–912. See <http://Chromatographyonline.com> (accessed 03/01/2017).
- Fredlund, D. G. (1976). Density and compressibility characteristics of air–water mixtures. *Can. Geotech. J.* **13**, No. 4, 386–396.
- Lee, K. L. & Black, D. K. (1972). Time to dissolve air bubble in drain line. *J. Soil Mech. Found. Div., ASCE* **98**, No. 2, 181–194.
- Makhnenko, R. Y. & Labuz, J. F. (2013). Saturation of porous rock and measurement of the B coefficient. In *Proceedings of the 47th US Rock Mechanics/Geomechanics Symposium San Francisco, CA, USA*, pp. 679–684. San Francisco, CA, USA: American Rock Mechanics Association.
- Najari, M. (2013). *A computational and experimental modelling of thermo-hydro-mechanical processes in a low permeability granite*. PhD thesis, McGill University, Montreal, QC, Canada.
- Selvadurai, A. P. S. (2000). *Partial differential equations in mechanics vol. 1. Fundamentals, Laplace's equation, diffusion equation, wave equation*. Berlin, Germany: Springer-Verlag.
- Wang, J. A. & Park, H. D. (2002). Fluid permeability of sedimentary rocks in a complete stress–strain process. *Engineering Geology* **63**, No. 3, 291–300.
- Wright, M., Dillon, P., Pavelic, P., Peter, P. & Nefiodovas, A. (2002). Measurement of 3-D hydraulic conductivity in aquifer cores at in situ effective stresses. *Ground Water* **40**, No. 5, 509–517.
- Zhang, L. (2013). Aspects of rock permeability. *Front. Struct. Civil Engng* **7**, No. 2, 102–116.

HOW CAN YOU CONTRIBUTE?

To discuss this paper, please submit up to 500 words to the editor at journals@ice.org.uk. Your contribution will be forwarded to the author(s) for a reply and, if considered appropriate by the editorial board, it will be published as a discussion in a future issue of the journal.